Book Chapter

Optimization in the Stripping Process of CO_2 Gas Using Mixed Amines

Pao Chi Chen* and Yan-Lin Lai

Department of Chemical and Materials Engineering, Lunghwa University of Science and Technology, Taiwan

*Corresponding Author: Pao Chi Chen, Department of Chemical and Materials Engineering, Lunghwa University of Science and Technology, 333, Taoyuan, Taiwan

How to cite this book chapter: Pao Chi Chen, Yan-Lin Lai. Optimization in the Stripping Process of CO_2 Gas Using Mixed Amines. In: Phattara Khumprom, Mladen Bošnjaković, editors. Advances in Energy Research. Hyderabad, India: Vide Leaf. 2020.

Conflicts of Interest: The authors declare no conflict of interest.

Abstract

The aim of this work was to explore the effects of variables on the heat of regeneration, the stripping efficiency, the stripping rate, the steam generation rate, and the stripping factor. The Taguchi method was used for the experimental design. The process variables were the CO2 loading (A), the reboiler temperature (B), the solvent flow rate (C), and the concentration of the solvent (monoethanolamine (MEA) + 2-amino-2-methyl-1-propanol (AMP)) (D), which each had three levels. The stripping efficiency (E), stripping rate ($\dot{m}_{CO_2}$), stripping factor (β), and heat of regeneration (Q) were determined by the mass and energy balances under a steady-state condition. Using signal/noise (S/N) analysis, the sequence of importance of the parameters and the optimum conditions were obtained, and the optimum operating conditions were further validated. The results showed that E was in the range of 20.98%–55.69%; $\dot{m}_{CO_2}$ was in the range of 5.57×10^{-5}–4.03×10^{-4} kg/s, and Q was in the range of 5.52–18.94 GJ/t. In addition, the S/N ratio analysis showed that the parameter sequence of importance as a whole was A > B > D > C, while the optimum conditions were A3B3C1D1, A3B3C3D2, and A3B2C2D2, for E, $\dot{m}_{CO_2}$, and Q, respectively. Verifications were also performed and were found to satisfy the optimum conditions. Finally, the correlation equations that were obtained were discussed and an operating policy was discovered.

Keywords

Heat of Regeneration; Stripping Rate; Stripping Factor; Mixed Solvent; Taguchi Method

Abbreviation

AMP-2-amino-2-methyl-1-propanol; AMPD-2-amino-2-methyl-propane-1,3-diol; DETA- Diethylenetriamine; MEA-Monoethanolamine; PZ- Piperazine; PZEA-(Piperazinyl-1)-2-ethylamine; SG- Sodium glycinate; S/N- Signal/Noise; TETA-Triethylenetetramine

Introduction

In order to reduce CO_2 gas emissions, many solutions have been proposed for several significant industries, such as coal-fired power plants, petroleum industries, steel industries, and cement industries. In this regard, a number of technologies have been applied, such as post-combustion, pre-combustion, oxyfuel combustion, and chemical looping. Among these technologies, an absorption-desorption process for post-combustion has been widely used [1]. A number of solvents have been adopted for the capture of CO_2 [2–4]. In these solvents, amines are most extensively used in chemical absorption to capture CO_2 [5–7]. As the chemical structure of an amine has at least one OH and amine group, the OH group can reduce the vapor pressure of the amine, and because an amine has alkaline properties, it can absorb acidic gases. Among the various amines, monoethanolamine (MEA) is used most extensively, because of its high solution absorbability, high alkalinity, high reaction rate, regenerability, and low cost. However, some drawbacks have been observed, such as high solvent regeneration energy, corrosion, and degradation.

Capturing CO_2 increases the cost of electricity production by 70%, while the energy required for the regeneration process is estimated to be in the range of 15%–30% of a power plant's output [8,9]. Therefore, effectively reducing the cost of electric power has become the key to the success or failure of carbon capture and sequestration (CCS). Achieving minimum heat for regeneration has become a significant challenge, especially for the improvement of the stripper structure, the discovery of new solvents, and improvements in operating conditions [10–20]. In the stripping process, rich solvents are heated in the stripper to

allow for the release of CO_2 from the scrubbed solutions. The stripping vapor, involving water vapor, CO_2, and small amounts of solvents, is regenerated in the reboiler, and rises from the reboiler through the column to the top of the stripper. The stripping vapor counter-current contacts a rich-loading feed stream, which absorbs energy from the stripping steam for CO_2 desorption. The remaining vapor is condensed at the top of the column in the overhead condenser. The vapor and liquid contact system are shown in Figure 1, indicating that the system is complex.

The heat of the solvent regeneration in the stripper of the CO_2 capture process can be described as follows [13,21]:

$$Q = Q_{sen} + Q_{abs} + Q_{vap} \qquad (1)$$

where Q_{sen} is the sensitive heat, Q_{vap} is the heat of evaporation, and Q_{abs} is the heat of absorption. In general, the three terms are evaluated separately when the relevant thermodynamic data are available.
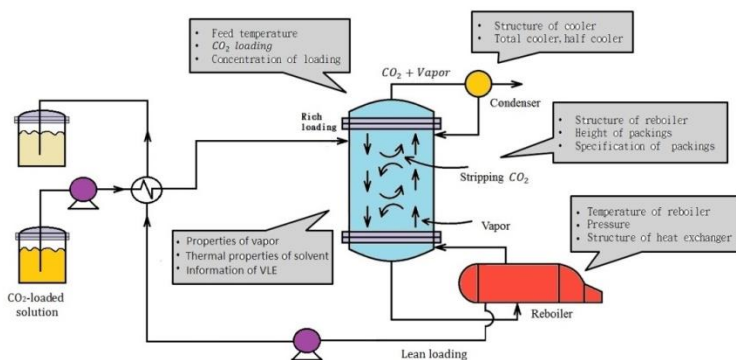

Figure 1: Vapor and liquid contact in the stripper.

The cost of regeneration is influenced by the adopted solvent, the stripping equipment structure, the operating temperature, and the steam cost [8,9,22,23]. In order to minimize the heat of regeneration, many studies have focused on more efficient

solvents that show a lower heat of absorption [14,24,25]. These studies showed that blended solvents have been widely studied in the capture of CO_2 gas [6,7,10], while new solvents have also been actively tested [11,14,20,26]. As a result, many scholars have studied blended amines and effective solvents, with the goal of improving regeneration energy [14–20]. Choi et al. [6] found that MEA + 2-amino-2-methyl-1-propanol (AMP) has a relatively high economic benefit. Some studies have indicated that if the gas stripping column uses a split-flow, the energy saved could be at least 20%. The effect of the stripper configuration on the heat duty was also reported by Rochelle [23], who found that the reduction in energy requirement was 5%–20%. Additionally, rich loading and lean loading each have a relative effect on heat duty. The findings showed that heat duty in regeneration is relatively higher when rich loading is low, whereas, a lean loading of 0.1–0.2 has a minimum heat duty [21]. Li and Keener [1] reported that many studies focus on reducing sensible heat and the heat of evaporation. In order to understand the contribution of individual heat duties, an investigation of the heat mechanism of regeneration energy can also be explored if the thermodynamic data are available. Table 1 shows the heat of regeneration data under various conditions. The reported levels for the heat of regeneration are in the range of 2.1–11.25 GJ/t, depending on the operating system. However, there are no available empirical equations that could be used to predict the heat of regeneration at the given conditions.

In some processes, the focus on the development of blended amines and new solvents for obtaining a low heat of absorption could be misleading, because the focus on solvents with a low heat of absorption is not reasonable without considering the overall process, as pointed out by Oexmann and Kather [21]. They found that at a low heat of absorption, the heat of the solvent regeneration at a low pressure leads to an increase in power for compression, as well as a lower quality steam. On the other hand, at a high heat of absorption, solvents show an increase in stripper operating pressure, and a reboiler temperature that leads to less water vapor at the stripper head. Thus, less heat must be provided in the reboiler. They also stated that in the evaluation of a solvent, it is necessary to consider the

interdependence of the three terms that contribute to the heat of regeneration and their connection to the process parameters. This could be accomplished by balancing the materials and energy in the stripper. However, the regeneration energies are related to the type of solvent, reboiler temperature, solvent flow rate, loading, and structure of the stripper. Therefore, understanding the parameter significance and optimization conditions in order to reduce regeneration energy needs was required. This could be done by using the Taguchi experimental design [4,5].

In this work, the process variables included the concentration of the solvents, the flow rate, the CO_2-loading, and the reboiler temperature. In order to better understand the effects of the process variables on the outcome data, a framework was designed. The stripping efficiency, heat of regeneration, stripping rate, and steam generation rate were calculated using materials and an energy balance model created with the aid of thermal data [2,15]. Finally, the data were used to make a regression to obtain empirical equations, which were then discussed further.

Table 1: Heats of regenerations and operating conditions at various systems. AMP—2-amino-2-methyl-1-propanol; SG—sodium glycinate; MEA—monoethanolamine.; AMPD—2-amino-2-methyl-propane-1,3-diol; DETA—Diethylenetriamine; PZ—Piperazine; PZEA—(Piperazinyl-1)-2-ethylamine; TETA—Triethylenetetramine

Solvents	Conditions	Heat of Regeneration (GJ/t-CO_2)	References
SG	Loading = 0.11–0.52 T = 100–120 °C 3–6 M SG	3.68–10.75	[4]
AMP + PZ	Loading = 0.46 L/G = 2.9 18 wt. % AMP + 17.5 wt. % PZ	3.4–4.4	[7]
DETA	Loading = 1.2–1.4 Solvent flow rate = 3–12 m^3/m^2-h 2–3 M DETA	2.61–4.96	[13]
ACOR100 (MEA + TETA + AMPD + PZEA)	Solvent flow rate = 0.4–0.8 L/min Partial pressure of CO_2 = 54 mbar	2.7–3.9	[24]
KoSol-4	Loading = 0.8 L/G = 1.4–3.1 kg/Sm^3 P = 0.35–0.8 kg/cm^2	3.0–4.1	[14]
SG	Loading = 0.13–0.50 15–40 wt. % L/G = 2–10 L/m^3	5.3–8.5	[26]
AMP	Loading = 0.55 30 wt. % AMP	2.1	[27]
MEA	Loading = 0.25–0.49 30 wt. % MEA	3.3–6.4	[28]
PZ	Loading 0.4 T=120-150 °C	2.93–3.43	[29]
Ammonia	Loading = 0.0525–0.01236 7%–14% Ammonia	11.25	[30]
MEA MEA + ionic liquid + water	30 wt. % MEA 30 wt. % + 40 wt. % + 30 wt. % T = 103 °C Simulation	8.19 5.14	[31]
SG MEA	30 wt. % T = 40–120 °C Thermodynamic calculation	5.7 4.7	[32]
MEA+AMP	MEA:AMP = 2:1/1:1/1:2 T = 103–110 °C	2.5–5.0	[10]

Experimental Features
Experimental Design

The experimental design had four parameters, namely: the concentration of blended amine (MEA + AMP), the feed rate, the CO_2 loading, and the reboiler temperature. Each parameter had three levels. Originally, MEA and AMP (30 wt.% AMP in total amine) were mixed together; then, the blended amines were poured into a known amount water to prepare the desired amine concentrations. Theoretically, 3^4 or 81 experiments were therefore needed. Using the Taguchi experimental design, the orthogonal array $L_9(3^4)$ showed nine experiments, thereby reducing the number of experiments needed and the research cost by over 80% [4,5]. The blended amine concentrations were 4 kmol/m^3, 5 kmol/m^3, and 6 kmol/m^3; the feed rates were 3×10^{-4}, 6×10^{-4}, and 9×10^{-4} m^3/s; the CO_2 loadings were 0.3, 0.4, and 0.5 kmol-CO_2/kmol-amine; and the reboiler temperatures were 100, 110, and 120 °C, respectively. The MEA/AMP weight fraction ratios obtained in here were 0.1908/0.0818, 0.2388/0.1023, and 0.2869/0.1229 for 4 kmol/m^3, 5 kmol/m^3, and 6 kmol/m^3, respectively. Table 2 shows the factors and levels in this work, while Table 3 presents the combination of experiments in the orthogonal array. The rich loading for the feed solution was obtained by early experimental preparation. Figure 2 illustrates the framework of the research project. The steps involved the input variables, the Taguchi experimental design, outcome data, data analysis, and verification.

Once the measured data were obtained, the experimental data could be evaluated, and the optimum condition and importance of the parameters could be determined with a signal/noise (S/N) ratio using the Taguchi analysis. The S/N ratio is calculated as follows:

$$(\frac{S}{N})_{SB} = -10 \times \log(\frac{1}{n}\sum_{i=1}^{n} z_i^2) \qquad \text{(smaller is better)} \qquad (1)$$

$$(\frac{S}{N})_{LB} = -10 \times \log(\frac{1}{n}\sum_{i=1}^{n} \frac{1}{z_i^2}) \qquad \text{(larger is better)} \qquad (2)$$

where, n is the amount of data, i is the amount of ith data, and z_i is the experimental data, as determined in this work.

Table 2: Factors and levels used in this study.

Factor	1	2	3
CO_2-loading(A) mol-CO_2/mol-amine	0.3	0.4	0.5
Reboiler temperature(B)/°C	100	110	120
Feed rate(C)/m^3/s	$3(10^{-4})$	$6(10^{-4})$	$9(10^{-4})$
Concentration of solvent (D)/kmol/m^3	4	5	6

Table 3: Orthogonal arrays for experimental design.

No.	A (kmol-CO_2/kmol-amine)	B (°C)	C (m^3/s)	D (kmol/m^3)
1	1	1	1	1
2	1	2	2	2
3	1	3	3	3
4	2	1	2	3
5	2	2	3	1
6	2	3	1	2
7	3	1	3	2
8	3	2	1	3
9	3	3	2	1

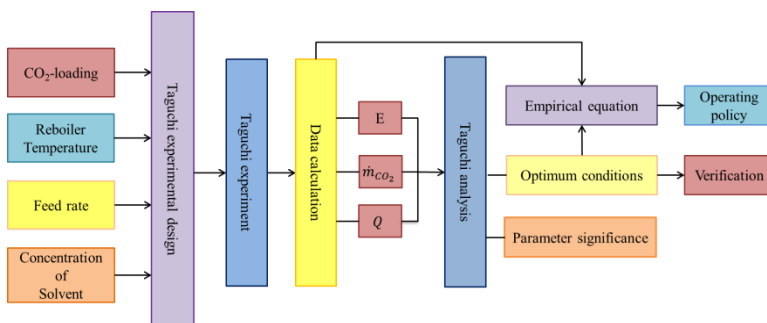**Figure 2:** A framework between the parameters and outcome data.

Experimental Device and Operating Procedure

The stripping system is shown in Figure 3. It included a packed column, a reboiler, a condenser, a heat exchanger, and a heating system. The diameter of the column was 50 mm. It was filled with an 8 × 8 mm θ-ring. The height of the packed column was 800 mm, and the height of the condenser was 500 mm. In

addition, a reboiler (12 L in volume) was heated by silicone oil using heating tubes. In order to adjust the pressure in the column, a pressure back valve was adopted as a suitable value at the top and bottom of the column, as shown.

In order to effectively explore the effect of the process variables on the performance of a stripper, a continuous process was adopted. First, the temperature indicators, cooling water circulator, and oil-bath power supply were switched on and adjusted to a preset temperature. Second, the prepared rich loading solution was poured into the reboiler until it flooded. When the oil-bath temperature reached the set temperature, the oil-bath pump power supply was turned on and an oil-bath inlet valve was used to adjust the flow. Third, the inlet temperature of the cooling water was set to the desired condition. Then, the reboiler was regulated to the desired experimental temperature. The experiment began when the temperature of the cooling water and that of the reboiler vapor temperatures reached the set temperatures. The rich loading in the storage tank flowed through a heat exchanger and into a packed bed, and contacted the vapor rising from the bottom of the column. The lean loading was withdrawn at the bottom of the reboiler and went through the heat exchanger, releasing the heat to the rich loading as the input solvent. The lean loading was withdrawn every 30 minutes for sample examination using a TOC (Total Organic Carbon) meter (Tekmar-Dohrmann Phoenix 800). The measurement procedure was performed according to the operation manual provided by Tekmar-Dohrmann Co. However, we need to prepare standard solutions (KHP and Na_2CO_3) before measurement. The analyzer needs to be calibrated every two-weeks. At this time, it requires being replaced with ultra-pure water. In addition, two antioxidant solutions also need to be replaced every month. One is a 20 wt.% H_2PO_4 solution and the other is one liter of 5 wt.% of H_2PO_4 solution dissolved with 10 g of $Na_2S_2O_8$ solids. In addition, the flow meter was calibrated using a measuring cylinder; then, it had a micro adjustment to a desired value. During the experiment, all of the temperature points indicated in Figure 3 had to be recorded, including the bed temperature (T01-T05). A combination of Taguchi experimental

designs was used to effectively explore the effect of multiple variables on the outcome data.
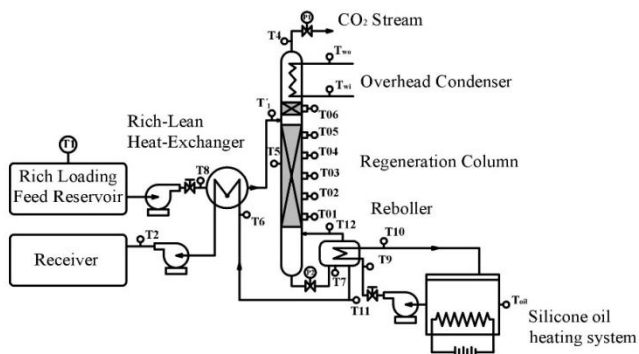

Figure 3: A stripping process used for both modes in this work.

T1:	Inlet temperature of rich loading	T7:	Reboiler temperature	T12:	Steam temperature
T2:	Temperature at outlet of heat exchanger	T8:	Inlet temperature of rich loading	T_{wi}:	Inlet temperature of cooling water
T4:	Out temperature at the top of cooler	T9:	Oil temperature at the inlet of reboiler (T_{in})	T_{wo}:	Outlet temperature of cooling water
T5:	Temperature of bed	T10:	Oil temperature at the outlet of reboiler (T_{out})	P1:	Pressure valve at the top of tower
T6:	Liquid temperature at the inlet of heat exchanger	T11:	Outlet temperature the reboiler	P2:	Pressure valve at the bottom of tower

Determination of Experimental Data

In order to obtain the experimental data, it was necessary to determine the materials and energy balances in the stripper, as shown in Figure 4. The data involving the stripping efficiency, stripping rate, heat of regeneration, and steam generation rate were calculated separately.
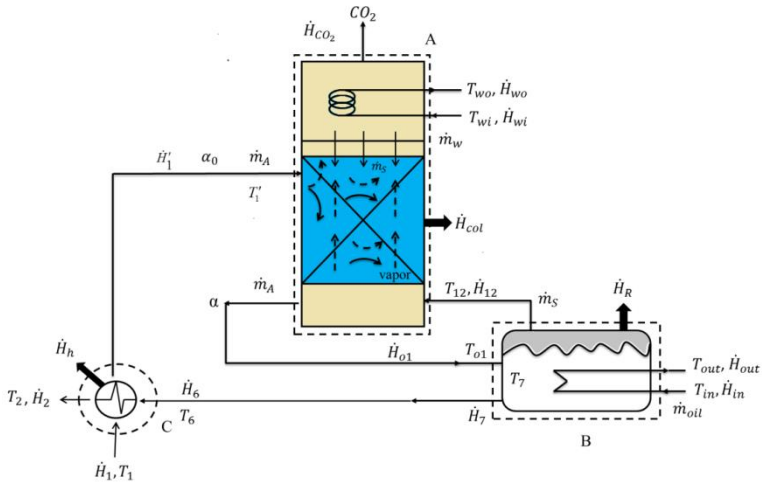
Figure 4: Materials and energy balances for the stripper.

Stripping Efficiency

The stripping efficiency is defined as the following:

$$E = \frac{\alpha_0 - \alpha}{\alpha_0} \times 100\% \tag{3}$$

where α_0 (mol-CO_2/mol-solvent) and α (mol-CO_2/mol-solvent) are the rich loading and lean loading, respectively.

Stripping Rate of CO_2

The stripping rate of CO_2 is defined as follows:

$$\dot{m}_{CO_2} = \dot{n}_A (\alpha_0 - \alpha) M_{CO_2} \tag{4}$$

where $\dot{n}_A$ (mol/s) is the molar rate of the solvent, and M_{CO_2} is the molecular weight of carbon dioxide.

Enthalpy Balance for Heat of Regeneration

From Figure 4, this procedure can be divided into three subsystems (i.e., A, B, and C), as indicated in the figure. Herein,

an enthalpy balance can be made at the steady state for the three subsystems, as shown below:

Subsystem A:

$$\dot{H}_{12} + \dot{H}_1' - \dot{H}_{01} - \dot{H}_{col} + \dot{H}_{wi} - \dot{H}_{wo} - \dot{H}_{CO_2} = 0 \tag{5}$$

Subsystem B:

$$\dot{H}_{in} - \dot{H}_{out} + \dot{H}_{01} - \dot{H}_7 - \dot{H}_{12} - \dot{H}_R = 0 \tag{6}$$

Subsystem C:

$$\dot{H}_6 + \dot{H}_1 - \dot{H}_2 - \dot{H}_1' - \dot{H}_h = 0 \tag{7}$$

From the three equations above, and assuming $\dot{H}_6 \approx \dot{H}_7$, it can be rewritten as the following equations:

$$\dot{H}_{CO_2} = \dot{H}_{reb} - \dot{H}_{loss} - (\dot{H}_2 - \dot{H}_1) - (\dot{H}_{wo} - \dot{H}_{wi}) \tag{8}$$

where

$$\dot{H}_{reb} = (\dot{H}_{in} - \dot{H}_{out}) = \dot{m}_{oil}\overline{C}_{p,oil}(T_{in} - T_{out}) \tag{9}$$

and

$$\dot{H}_{loss} = \dot{H}_R + \dot{H}_{col} + \dot{H}_h \tag{10}$$

and

$$\dot{H}_2 - \dot{H}_1 = \dot{m}_A\overline{C}_{pA}(T_2 - T_1) \tag{11}$$

And

$$\dot{H}_{wo} - \dot{H}_{wi} = \dot{m}_w\overline{C}_{pw}(T_{wo} - T_{wi}) \tag{12}$$

As $\dot{H}_{CO_2} = \dot{m}_{CO_2}Q$, Equation (8) becomes the following:

$$Q = \frac{\dot{H}_{reb} - \dot{H}_{loss} - (\dot{H}_2 - \dot{H}_1) - (\dot{H}_{wo} - \dot{H}_{wi})}{\dot{m}_{CO_2}} \tag{13}$$

where, $\dot{m}_{oil}$ is the mass flow rate of oil, $\overline{C}_{p,oil}$ is the mean heat capacity of oil, and T_{in} and T_{out} are the input and output

temperatures of the oil, respectively. In addition, $\dot{H}_{loss}$ is the heat loss, including $\dot{H}_{col}$ in the column, $\dot{H}_h$ in the heat exchanger, and $\dot{H}_R$ in the reboiler. Therefore, the heat losses $\dot{H}_{col}$, $\dot{H}_R$, and $\dot{H}_h$, which can easily be calculated separately, can be evaluated from the sensitive heat, while the heat transfer coefficient can be estimated by free convection [33]. Equation (13) states that the heat of regeneration can be determined when the enthalpy of the reboiler, the enthalpy of the heat loss, the enthalpy change between the inlet and outlet in the whole system, and the enthalpy change of the cooler are given.

Steam Flow Rate

In order to determine the bulk steam flow rate, materials and energy balances are required when the temperature of the stripper is fixed (Figure 4). Considering Subsystem B, the enthalpy balance at a steady state becomes the following:

$$\dot{H}_{12} = \dot{H}_{in} - \dot{H}_{out} + \dot{H}_{01} - \dot{H}_7 - \dot{H}_R \tag{14}$$

Equation (14) can be integrated into the following equation:

$$\dot{m}_s = \frac{\dot{m}_{oil}\overline{C}_{P,oil}(T_9 - T_{10}) - \dot{m}_A\overline{C}_{PA}(T_7 - T_{01}) - \dot{H}_R}{\Delta H^{vap}} \tag{15}$$

From the measured data and thermodynamic data [34], the steam flow rate can be evaluated.

Results and Discussion
Steady State Operation

The change in temperature at individual points, as indicated in Figure 3, was observed and recorded during the operation. Several important points, such as T1, T2, T6, T7, and T12, were recorded for No. 1, as shown in Figure 5. It was found that the temperatures remained constant when the operating time was

greater than 80 min. In addition, the distribution of the lean loading was found, as shown in Figure 6, which also remained constant after 80 min, which was coincident with Figure 5. In addition, the temperature distribution in the packed bed was recorded, as shown in Figure 7. The distributions approached a steady-state operation after 80 min, except for T05, as it was near the location of the solvent input and was prone to perturbation during operation. On the other hand, the effect of the solvent input on other points (T01 to T04) were weak, because they are far from the solvent input. Because of this, it could be said that the system changed to a steady state operation after 80 min. Under a steady state condition, the outcome data could be evaluated using Equations (3), (4), (13), and (15), as shown in Table 4, for the Taguchi experiments (No. 1–No. 9). In addition, the verification data of the optimum conditions are listed in this table, including No. 10, 11, and 12, which were discussed further. It was found that the data ranges for the Taguchi experiments were 20.96%–55.69%, 5.57×10^{-5}–4.03×10^{-4} kg/s, 5.52–18.94 GJ/t, 0.0580–0.203 kg-CO_2/kg-steam, and 8.38×10^{-4}–30.63×10^{-4} kg/s for E, $\dot{m}_{CO_2}$, Q, β, and $\dot{m}_s$, respectively. Except for No. 1 and 3, the values of Q fell between the data (2.1–11.5 GJ/t), as presented in Table 1. However, some data, such as that of no. 11 and 12, were comparable with the data [7,14,24,29] listed in Table 1 for the systems of MEA, ACOR100, Kosol-4, and AMP + PZ. However, the heat of the generation data shown here was higher than that reported by Aroonwilas and Veawab [10]. A possible reason was the difference in heating systems; the former was an oil bath system and the latter was a steam heating system. This could be seen in Equations (9) and (13). In order to reduce the heat of regeneration, it was necessary to choose a lower heat capacity oil that could reduce the $\dot{H}_{reb}$, as shown in Equation (13).
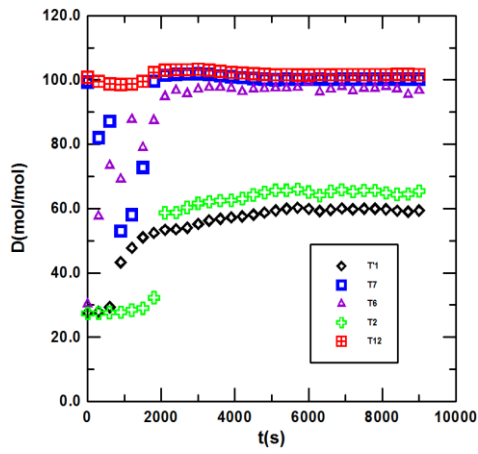
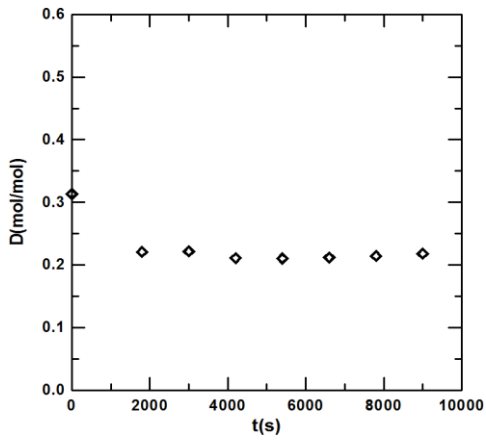**Figure 5:** Variations of temperature during operation.
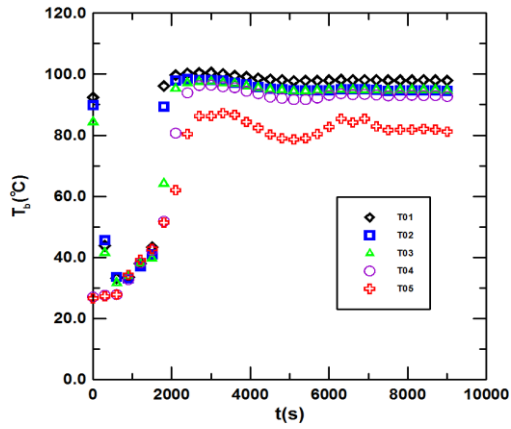

Figure 6: A plot of lean loading versus time.

Figure 7: Various temperature distributions in the packed bed.

Table 4: Measured data obtained in this work.

No.	α_0 $(\frac{kmol - CO_2}{kmol - amine})$	α $(\frac{kmol - CO_2}{kmol - amine})$	t_R (°C)	C_A (kmol/m³)	$Q_A (10^4)$ (m³/s)	Q (GJ/t)	$\dot{m}_{CO_2}$ (10^{-5} kg/s)	$\dot{m}_s$ (10^{-4} kg/s)	β $(\frac{kg - CO_2}{kg - steam})$	E (%)
1	0.31	0.22	100	4	3	15.69	5.57	8.82	0.063	30.43
2	0.31	0.24	110	5	6	7.29	10.04	8.38	0.120	22.45
3	0.30	0.22	120	6	9	18.94	16.71	30.63	0.058	20.98
4	0.41	0.30	100	6	6	10.05	16.71	12.34	0.144	23.64
5	0.41	0.25	110	4	9	7.52	28.91	14.52	0.199	40.79
6	0.39	0.13	120	5	3	6.75	15.77	9.06	0.174	54.78
7	0.51	0.34	100	5	9	7.69	40.26	20.67	0.195	35.73
8	0.50	0.25	110	6	3	7.08	21.59	10.62	0.203	49.63
9	0.49	0.18	120	4	6	5.52	32.04	17.21	0.186	55.70
10	0.55	0.21	120	4	3	6.89	17.41	7.10	0.245	58.18
11	0.47	0.26	120	5	9	3.97	46.15	19.24	0.236	44.54
12	0.52	0.31	110	5	6	4.44	29.61	13.14	0.225	39.20

Taguchi Analysis
S/N Ratio for E

The stripping efficiency for the nine data points was analyzed according to the S/N ratio, and the results are shown in Table 5. The parameters, in order of importance, were A > D > C > B, while the optimum condition was A3B3C1D1. Similarly, the same analysis for $\dot{m}_{CO_2}$ and Q were obtained and are listed in Table 6. It was found that the effects of parameters A and D were significant, while those of B and C were minor. The verification of the optimum conditions for the three runs could thus be carried out further.

Table 5: Signal to noise (S/N) ratio analysis, as indicated in Equation (2), for efficiency (E).

Level	A	B	C	D
1	27.71	29.40	32.78	32.26
2	31.49	31.05	29.80	30.95
3	33.30	32.04	29.90	29.27
Delta	5.59	2.64	2.98	2.99
Rank	1	4	3	2

Table 6: S/N ratio analysis to obtain optimum condition and parameter significance.

S/N	Optimum condition	Parameter importance
E (Equation (2))	A3B3C1D1	A > D > C > B
$\dot{m}_{CO_2}$ (Equation (2))	A3B3C3D2	A > C > B > D
Q (Equation (1))	A3B2C2D2	A > D > B > C

Confirmation of the Optimum Conditions

The procedure of confirmation was similar to that reported in Section 2.2. The results of the confirmation tests for the three optimum conditions are listed in Table 7. The words printed in red are the optimum values obtained here compared with the Taguchi experimental values, as shown in Table 4. The results indicated that the Taguchi experimental design for this study was reliable. In order to verify the optimum data, the Taguchi data together with the three optimum sets of data were all adopted for regression.

Table 7: Confirmation of optimum conditions.

No	Optimum Condition	E (%)	$\dot{m}_{CO_2}$ ($\times 10^5$) (k g/s)	Q (G J/t)
No. 10	A3B3C1D1	(58.18)	17.41	6.89
No. 11	A3B3C3D2	44.54	(46.15)	3.97
No. 12	A3B2C2D2	39.20	29.61	(4.44)

Empirical Equations

In order to obtain the empirical equations for E, $\dot{m}_{CO_2}$, Q, and $\dot{m}_s$, the experimental data were correlated with suitable parameters, that is, $\Phi = f(\alpha_0, t_R, C_A, Q_A)$. For example, the stripping efficiency was correlated with the CO_2 loading, the reboiler temperature, the solvent concentration, and the flow rate. A total of twelve data sets (listed in Table 3) were used, and the results are as follows:

$$E = 1.94 \times 10^5 \exp(-\frac{3702.14}{T_R(K)}) \alpha_0^{0.68} [C_A(kmol/m^3)]^{-1.39} [Q_A(m^3/s)]^{-0.33} \quad (16)$$

The root means relative error, based on the measured values for Equation (16), was 4.97%. However, the R^2 obtained in here was 0.72. Figure 8 shows the confidence of the regression. It was found that most data, including the data for the optimum condition, were within a $\pm 20\%$ margin of error, showing that the regression was good. From Arrhenius' law, the temperature dependence of the correlation, such as Equation (16), was determined by the activation energy and temperature level of the correlation, as shown in this equation [35]. The activation energy obtained was found to be 30.78kJ/mol. The same regression procedure was performed in the others' correlation equations. The results for the stripping rate, steam flow rate, and heat of regeneration are shown below:

$$\dot{m}_{CO_2} = 2.08 \times 10^7 \exp(-\frac{1542.05}{T_R(K)}) \alpha_0^{2.03} [C_A(kmol/m^3)]^{-0.23} [Q_A(m^3/s)]^{0.68} \quad (17)$$

$$\dot{m}_s = 1.44 \times 10^8 \exp(-\frac{2985.14}{T_R(K)}) \alpha_0^{-0.097} [C_A(kmol/m^3)]^{0.19} [Q_A(m^3/s)]^{0.78} \quad (18)$$

and

$$Q = 0.10\exp(\frac{895.75}{T_R(K)})\alpha_0^{-1.45}\alpha^{-0.0083}[C_A(kmol/m^3)]^{0.35}[Q_A(m^3/s)]^{-0.011} \tag{19}$$
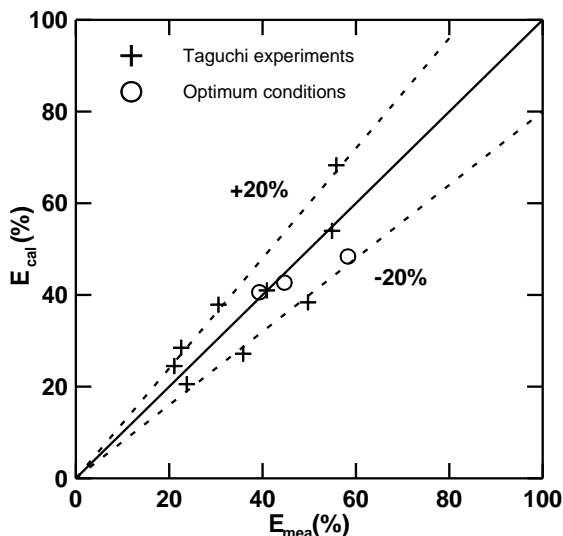

.
Figure 8: A plot of E_{cal} versus E_{mea}, showing the data distribution.

It was found that most data, including the data for the optimum conditions, were within a ±20% margin of error for the stripping rate, steam flow rate, and heat of regeneration, as shown in Figures 9–11, showing that the regressions were good. However, Figure 11 shows that some data were scattered beyond the ±20% margin of error. The regression errors for the four correlations are listed in Table 8, and were in the range of 4.79–7.91. The activation energy for the four equations is also listed in this table, in which the range was −7.45–30.78 kJ/mol. The negative value for Q means that Q decreased with the increase in T. Correlations with high activation energies are temperature-sensitive; correlations with low activation energies are very temperature-insensitive [35]. Therefore, E was more temperature-sensitive compared with other outcome data. In addition, the exponents of each of the equation is also listed in this table for comparison. The results showed that the effect of α_0

on $\dot{m}_{CO_2}$ was obvious as compared with others, while the effect of C_A on E was the most significant. Finally, the effect of Q_A on $\dot{m}_s$ was more significant, compared with the others' correlations. In addition, the exponents and activation energy for E and Q were in contract. They need to be discussed in later works.
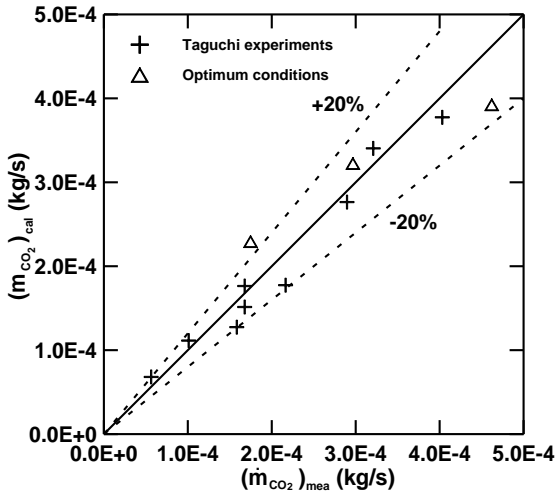

Figure 9: A plot of the calculated stripping rate versus the measured stripping rate.
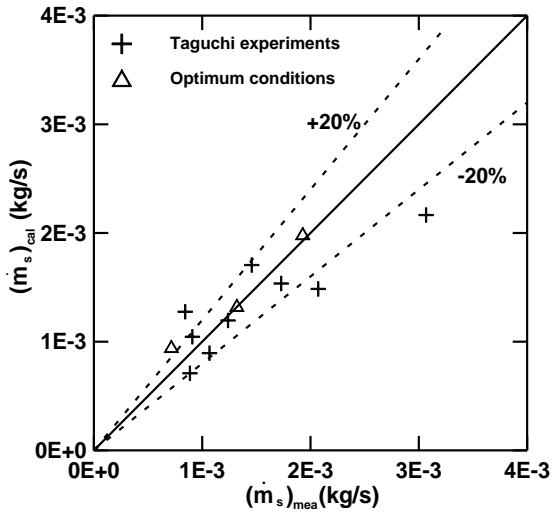
Figure 10: A plot of calculated steam generation rate versus measured values.
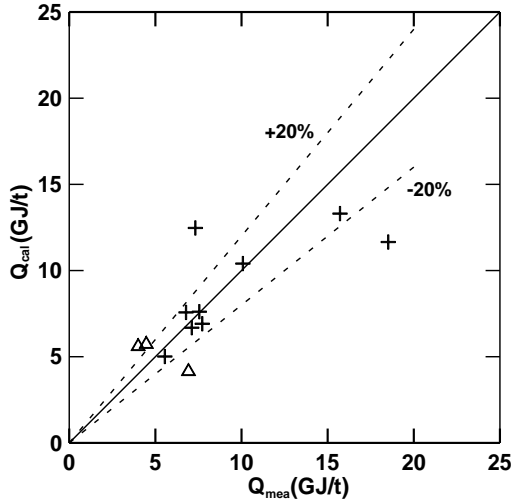

Figure 11: A plot of calculated and measured data for *Q*, showing regression error.

Table 8: The root mean relative error, activation energy, and exponent for Equations (16)–(19).

Outcome data	Root mean relative error (%)	Activation energy (kJ/mol)	Exponent for each equation		
			α_0	C_A	Q_A
Equation 16 (E)	4.97 ($R^2 =$ 0.72)	30.78	0.68	−1.39	−0.33
Equation 17 ($\dot{m}_{CO_2}$)	7.00 ($R^2 =$ 0.92)	12.82	2.03	−0.23	0.68
Equation 18 ($\dot{m}_s$)	5.71 ($R^2 =$ 0.71)	24.81	−0.097	0.19	0.78
Equation 19 (Q)	7.91 ($R^2 =$ 0.56)	−7.45	−1.45	0.35	−0.011

Heat of Regeneration and Stripping Factor

Alternatively, the heat of regeneration was used to correlate to the stripping factor, which was defined as the ratio of the stripping rate to the steam flow rate, that is, $\beta = \dot{m}_{CO_2} / \dot{m}_s$. Here, the β value can act as the performance indicator of the stripper. The higher the β value, the better the stripper. Thus, the regression result became the following:

$$Q = 1.62\beta^{-0.84} \tag{20}$$

The R-square value was 0.8036. Figure 12 shows a plot of Q versus β. It was found that the trend of the Q value decreased with the increase in β, which could be calculated using Equations (17) and (18) when α, Q_A, C_A, and T_R were given. The increase in β indicated that, with the same amount of steam, more CO_2 could be desorbed.

Figure 12. A plot of Q against β, showing the effect of the stripping factor on the heat of regeneration.

Policy in Operation

Figure 13 is a plot of E versus Q. The plot shows that the trend of E decreased with the increase in Q. Therefore, if Q was set to 3, the corresponding stripping efficiency would be about 80%. From Equation (16), it was found that α_0 and t_R needed to be higher, while C_A and Q_A needed to be lower. On the other hand, when ignoring the effects of the lean CO_2 loading and liquid flow rate shown in Equation (19) for Q, it was found that α_0 and t_R needed to be higher, while C_A needed to be lower. The trend was similar to that obtained from Equation (16) for E. Because of these findings, α_0 and t_R needed to be controlled at higher values, while lower values for C_A and Q_A required reducing the Q value and increasing the E value.
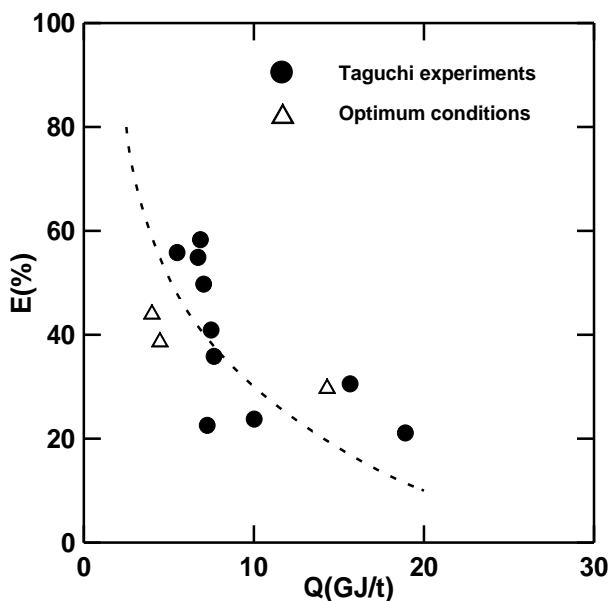
Figure 13: A plot of *E* versus *Q* showing the variation of *E* with *Q*.

Conclusions

This study successfully used a continuous packed-bed stripper with an MEA + AMP solvent containing CO_2 for the study of the heat of regeneration using the Taguchi experimental design. Using mass and energy balances, the stripping efficiency, stripping rate, steam flow rate, stripping factor, and heat of regeneration could be determined under a steady-state condition. Quantitatively, the effects of the variables on E, $\dot{m}_{CO_2}$, β, and Q were explained by the empirical equations obtained in this study. The definition of the stripping factor (β) was used to describe the performance of the stripper. It was found that the heat of regeneration could be correlated with β. The heat of regeneration decreased with the increase in β, showing that more CO_2 could be desorbed. The Taguchi S/N ratio analysis found that the parameter importance sequence was A > D > B > C. Additionally, the optimum conditions for E, $\dot{m}_{CO_2}$, and Q were all verified, thereby showing confidence in the experimental

design. In order to obtain a higher E and a lower Q, lower values of Q_A and C_A were required, while higher values of α_0 and t_R were needed.

References

1. Li T, Keener TC. A review: Desorption of CO_2 From Rich Solutions in Chemical Absorption Processes. Int. J. Greenh. Gas Control. 2016; 51: 290–304.
2. Aronu UE, Svendsen HF, Hoff KA, Juliussen O. Solvent Selection for Carbon Dioxide Absorption. Energy Procedia. 2009; 1: 1051–1057.
3. Adeosun A, Goetheer NEH, Abu-Zahra MRM. Absorption of CO_2 by Amine Blends Solution: An Experimental Evaluation. Int. J. Eng. Sci. 2013; 3: 12–23.
4. Chen PC, Lin SZ. Optimization in the Absorption and Desorption of CO_2 Using Sodium Glycinate Solution. Appl. Sci. 2018; 8: 2041.
5. Chen PC, Luo YX, Cai PW. Capture of Carbon Dioxide Using Monoethanolamine in a Bubble-Column Scrubber. Chem. Eng. Technol. 2015; 38: 274–282.
6. Choi WJ, Seo JB, Seo SY, Jung JH, Oh KJ. Removal Characteristics of CO_2 Using Aqueous MEA/AMP Solutions in the Absorption and Regeneration Process. J. Environ. Sci. 2009; 21: 907–913.
7. Dash SK, Sammanta N, Bandyopadhyay SS. Simulation and Parametric Study of Post Combustion CO_2 Capture Process Using (AMP+PZ) Blended Solvent. Int. J. Greenh. Gas Control. 2014; 21: 130–139.
8. Leung DYC, Caramanna G, Maroto-Valer MM. An Overview of Current Status of Carbon Dioxide Capture and Storage Technologies. Renew. Sustain. Energy Rev. 2014; 39: 426–443.
9. Ho MT, Allinson GW, Wiley DE. Comparison of MEA Capture Cost for Low CO_2 Emissions Sources in Australlia. Int. J. Greenh. Gas Control. 2011; 5: 49–60.
10. Aroonwilas A, Veawab A. Integration of CO_2 Capture Unit Using Blended MEA-AMP Solution into Coal-Fired Power Plants. Energy Procedia. 2009; 1: 4315–4321.

11. Kim JH, Lee JH, Lee IY, Jang KR, Shim JG. Performance Evaluation of Newly Developed Absorbents for CO_2 Capture. Energy Procedia. 2011; 4: 81–84.
12. Han K, Ahn CK, Lee MS. Performance of an Ammonia-Based CO_2 Capture Pilot Facility in Iron and Steel Industry. Int. J. Greenh. Gas Control. 2014; 27: 239–246.
13. Zhang X, Fu K, Liang Z, Yang Z, Rongwong W, et al. Experimental Studies of Regeneration Heat Duty for CO_2 Desorption from Aqueous DETA Solution in a Randomly Packed Column. Energy Procedia. 2014; 63: 1497–1503.
14. Kwak NS, Lee JH, Lee IY, Jang KR, Shim JG. A Study of New Absorbent for Post-Combustion CO_2 Capture Test Bed. J. TIChE. 2014; 45: 2459–2556.
15. Xiao J, Li CC, Li MH. Kinetics of Absorption of Carbon Dioxide into Aqueous Solutions of 2-amino-2-methyl-1-propanol+Monoethanolamin. Chem. Eng. Sci. 2000; 55: 161–175.
16. Kumar PS, Hogendoorn JA, Versteeg GF, Feron PHM. Kinetics of the Reaction of CO_2 With Aqueous Potassium Salt of Taurine and Glycine. Aiche J. 2003; 49: 203–213.
17. Singh P, Versteeg GF. Structure and Activity Relationships for CO_2 Regeneration from Aqueous Amine-Based Absorbents. Process Saf. Environ. Prot. 2008; 86: 347–359.
18. Idem R, Wilson M, Tontiwachwuthikul P, Chakma A, Veawab A, et al. Pilot Plant Studies of the CO_2 Capture Performance of Aqueous MEA and Mixed MEA/MDEA Solvents at the University of Regina CO_2 Capture Technology Development Plant and Boundary Dam CO_2 Capture Demonstration Plant. Ind. Eng. Chem. Res. 2006; 45: 2414–2420.
19. Weiland RH, Hatcher NA. Post-Combustion CO_2 Capture with Amino-Acid Salts. In Proceedings of the GPA Europe Meeting. Lisbon, Portugal. 2010.
20. Lin PH, Shan D, Wong H. Carbon Dioxide Capture and Regeneration with Amine/Alcohol/Water. Int. J. Greenh. Gas Control. 2014; 26: 69–75.
21. Oexmann J, Kather A. Minimising the Regeneration Heat Duty of Post-Combustion CO_2 Capture by Wet Chemical Absorption: The Misguided Focus on Low Heat of

Absorption Solvents. Int. J. Greenh. Gas Control. 2010; 4: 36–43.

22. Veawab V, Aroonwilas A. Energy Requirement for Solvent Regeneration in CO_2 Capture Plants. In Proceedings of the 9th International CO_2 Capture Network. Copenhagen, Denmark. 2006.

23. Rochelle GT. Innovative Stripper Configurations to Reduce the Energy Cost of CO_2 Capture. In Proceedings of the Second Annual Carbon Sequestration Conference. Alexandria, VA, USA. 2003.

24. Esmaeili H, Roozbehani B. Pilot-Scale Experiments for Post-Combustion CO_2 Capture from Gas Fired Power Plants with a Novel Solvent. Int. J. Greenh. Gas Control. 2014; 30: 212–215.

25. Yu CH, Huang CH, Tan CS. A Review of CO_2 Capture by Absorption and Adsorption. Aerosol Air Qual. Res. 2012; 12: 745–769.

26. Rabensteiner M, Kinger G, Koller M, Gronald G, Unterberger S, et al. Investigation of the Suitability of Aqueous Sodium Glycinate as a Solvent for Post Combustion Carbon Dioxide Capture on the Basis of Pilot Studies and Screening Methods, Int. J. Greenh. Gas Control. 2014; 29: 1–3.

27. Ali Khan A, Halder GN, Saha AK. Carbon Dioxide Capture Characteristics from Flue Gas Using Aqueous 2-amino-2-methyl-1-propanal (AMP) and Monoethanolamine (MEA) Solutions in Packed Bed Absorption and Regeneration Columns. Int. J. Greenh. Gas Control. 2015; 32: 15–23.

28. Badea AA, Dinca CF. CO_2 Capture from Post-Combustion Gas by Employing MEA Absorption Process— Experimental Investigation for Pilot Studies. U.P.B. Sci. Bull. Ser. D 2012; 74: 21–32.

29. Van Wagener DH, Rochelle GT. Stripper Configuration for CO_2 Cpature by Aqueous Monoethhanolamine and Piperazine, Energy Procedia. 2011; 4: 1323-1330.

30. Yeh JT, Resnik KP, Rygle K, Pennline HW. Semi-Batch Absorption and Regeneration Studies for CO_2 Capture by Aqueous Ammonia. Fuel Process. Technol. 2005; 86: 1533–1546.

31. Yang J, Yu X, Yan J, Tu ST. CO_2 Capture Using Solution Mixed with Ionic Lliquid. Ind. Eng. Chem. Res. 2014; 53: 2790–2799.
32. Song HJ, Lee S, Park K, Lee J, Chand Spah D, et al. Simplified Estimation of Regeneration Energy of 30 wt% Sodium Glycinate Solution for Carbon Dioxide Absorption. Ind. Eng. Chem. Res. 2008; 47: 9925–9930.
33. Geankoplis CJ. Transport Processes and Unit Operations. Boston: Allyn and Bacon, Inc. 1983; 244-250.
34. Smith JM, van Ness HC, Abbott MM. Introduction to Chemical Engineering Thermodynamics. New York: McGraw Hill. 2006; 116–125.
35. Levenspiel O. Chemical Reaction Engineering. Hoboken: Jon Wiley & Sons, Inc. 1999; 28–29.

Nomenclature

C   kmol/m^3 concentration

C_A kmol/m^3 concentration of amine

C_{Pw} kJ/kg·K   hat capacity of water

C_{PA} kJ/kg·K   hat capacity of amine

$C_{p,oil}$ kJ/kg·K   hat capacity of oil

E   %   stripping efficiency

$\dot{H}R$

   kJ/s   reboiler heat loss

$\dot{H}col$

   kJ/s   column heat loss

$\dot{H}cold$

   kJ/s   heat removed by cooler

H_h kJ/s   heat exchanger heat loss

H^{vap} kJ/kg   heat of evaporation

$\dot{H}loss$

   kJ/s   total heat loss

$\dot{H}reb$

   kJ/s   heat flow rate in reboiler

$\dot{H}1$

   kJ/s   enthalpy at inlet

$\dot{H}2$

   kJ/s   enthalpy at outlet

H_{abs} kJ/kg   heat of absorption

$\dot{m}CO2$

   kg/s   stripping rate

$\dot{m}oil$

   kg/s   oil flow rate

$\dot{m}s$

   kg/s   steam generation rate

$\dot{m}w$

	kg/s	cooling water flow rate
n	-	number of data points
$\dot{n}A$	kmol/s	amine flow rate
Q	W	total heat flow
Q_A	m^3/s	liquid volumetric flow rate
Q_{abs}	kW	heat flow of absorption
Q_{sen}	kW	sensitive heat flow
Q_{vap}	W	heat flow of evaporation
T_{in}	K	temperature at inlet of reboiler
T_{out}	K	temperature at outlet of reboiler
T_{o1}	K	temperature at the bottom of column
T_R	K	reboiler temperature
T_s	K	steam temperature
T_{wi}	K	inlet temperatureof the cooler
T_{wo}	K	outlet temperatureof the cooler
T_1	K	temperature at inlet of storage tank
t_R	°C	reboiler temperature
z_i	-	value of ith data

Greek Letters

α	kmol-CO_2/kmol-amine	rich loading
α_0	kmol-CO_2/kmol-amine	lean loading
β	kg-CO_2/kg-steam	stripping factor